Neocortical Synchronized Oscillations Induced by Thalamic Disinhibition *In Vivo*

Manuel A. Castro-Alamancos

Department of Neurology and Neurosurgery, Montreal Neurological Institute, McGill University, Montreal, Quebec H3A2B4 Canada

Thalamocortical circuits are recognized as the main elements involved in the genesis of synchronized oscillations typical of certain generalized seizures. We addressed the capability of thalamic disinhibition to generate synchronized oscillations in neocortex. Microdialysis was used to infuse $GABA_A$ and $GABA_B$ receptor antagonists directly into the thalamus of anesthetized rats while recording cortical field potentials from 16 sites aligned perpendicular to the cortical surface, using 100 μm spaced linear array silicon probes. The results demonstrate that block of thalamic $GABA_A$ receptors induces continuous 3 Hz discharges in neocortex and that thalamic $GABA_B$ receptors mediate this activity. Also, during thalamic disinhibition sporadic long-lasting discharges at 12 Hz occur that do not depend on $GABA_B$ receptors. Current source density analysis of these activities revealed that the dynamics of sinks and sources for the 3 and 12 Hz discharges was quite distinct, in a way that suggests a different active involvement of the neocortex. The results indicate that intrathalamic inhibitory processes play an essential role in the generation of neocortical synchronized oscillatory activity that may be related to certain forms of generalized seizures.

Key words: epilepsy; seizure; oscillations; thalamus; neocortex; GABA

Widespread synchronous activity characterizes the electroencephalogram of humans during several types of generalized seizures (Jasper and Kershman, 1941). Since the early work of Jasper, much evidence has supported an essential role of the thalamus in the generation of generalized activity. In particular, evidence from rat genetic models of absence epilepsy has provided abundant support for a thalamic involvement in the genesis of generalized discharges (Buzsaki et al., 1988; Vergnes et al., 1990).

Another widely used model of generalized activity, the feline generalized penicillin model, has provided at best ambivalent support for the involvement of the thalamus. In this model, the $GABA_A$ receptor antagonist, penicillin, is injected parenterally. The result is the occurrence of bilaterally synchronous discharges at ~3 Hz (Prince and Farrell, 1969; Gloor et al., 1990). The immediate question was where is the penicillin acting, the thalamus or the neocortex? Early work had shown that penicillin infusion into the thalamus alone produced the transformation of 10 Hz spindle oscillations to 3 Hz discharges in barbiturate-anesthetized animals (Ralston and Ajmone-Marsan, 1956). However, a subsequent study indicated that thalamic infusion of penicillin was ineffective in producing 3 Hz discharges. Instead, diffuse cortical application of the drug was capable of producing this activity without any thalamic participation (Gloor et al., 1977). A latter revision of these results concluded that the lack of effect of thalamic penicillin was "inconclusive" and that the lack of participation of thalamic circuits after diffuse cortical penicillin was "erroneous" (Gloor et al., 1990). This resulted in the attribution of a more active role to the thalamus in the generation of 3 Hz activity. Accordingly, the resulting hypothesis was that thalamic spindle oscillations are transformed into synchronous discharges through an increased cortical excitability (Gloor and Fariello, 1988; Gloor et al., 1990). More recent work both using slices and anesthetized cats has shown that application of a $GABA_A$ receptor antagonist into the thalamus slows thalamic spindle oscillations from 10 to ~3 Hz (von Krosigk et al., 1993) but does not seem to induce seizures (Steriade and Contreras, 1998).

The present study further describes the effects of blocking thalamic GABA receptors on spontaneous neocortical activity *in vivo*, as well as on the pattern of spatial (laminar) spread of neocortical activity revealed by current source density analysis. We found that blockade of thalamic $GABA_A$ receptors produces two different forms of synchronized oscillatory activity in neocortex: (1) continuous waxing and waning synchronized oscillations at 3 Hz that depend on thalamic $GABA_B$ receptors and (2) sporadic synchronized oscillations at 12 Hz that do not depend on

Received June 7, 1999; revised July 15, 1999; accepted July 21, 1999.

This work was supported by the Medical Research Council of Canada, Fonds de la Recherche en Sante du Quebec, and McGill University Research Development Fund. Thanks to Drs. Gyorgy Buzsaki and Mircea Steriade for helpful comments on this manuscript. Special thanks to the Center for Neural Communication Technology (University of Michigan) and Jamie Hetke for providing the silicon probes and helpful support. Thanks to Novartis for providing CGP35348

Correspondence should be addressed to Dr. Manuel Castro-Alamancos, Montreal Neurological Institute, 3801 University Street, Room WB210, Montreal, Quebec H3A 2B4 Canada.

This article is published in *The Journal of Neuroscience*, Rapid Communications Section, which publishes brief, peer-reviewed papers online, not in print. Rapid Communications are posted online approximately one month earlier than they would appear if printed. They are listed in the Table of Contents of the next open issue of JNeurosci. Cite this article as: JNeurosci, 1999, 19:RC27 (1–7). The publication date is the date of posting online at www.jneurosci.org.

http://www.jneurosci.org/cgi/content/full/3493

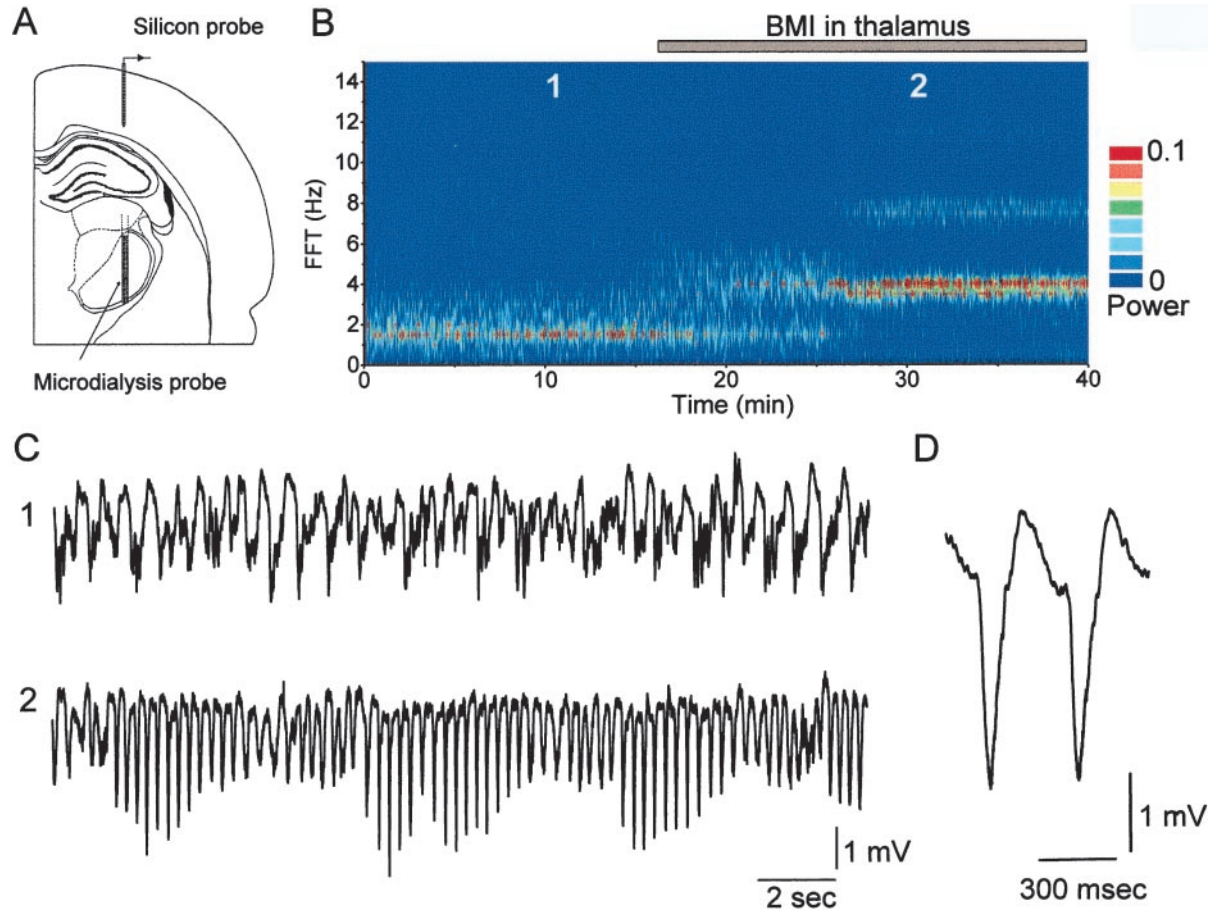

Figure 1. Effect of blocking thalamic $GABA_A$ receptors on neocortical field potential activity. *A*, Schematic diagram depicting the locations of the microdialysis probe used to infuse drugs into the thalamus, and of the 16-site linear array silicon probe used to record activity from the neocortex. The silicon probe was located 3 mm more anterior than the microdialysis probe, but for simplicity they are shown in the same section. *B*, Power spectrum derived from every 2 sec of spontaneous field potential activity recorded from the neocortex and displayed as a color-contour plot. During infusion of ACSF through the microdialysis probe, neocortical activity consists of slow-wave activity. Infusion of a $GABA_A$ receptor antagonist (BMI) into the thalamus results in the abolishment of this activity, which is transformed into a robust 3 Hz activity. *C*, Examples of recordings before and during BMI application. The numbers on the traces correspond to the times indicated in *B*. Recordings were from a site 1 mm in depth from the surface. Traces are 20 sec long. *D*, Electrographic pattern of the 3 Hz activity induced in the neocortex by BMI, which consists of a negative spike followed by a positive wave.

thalamic $GABA_B$ receptors. Both forms of synchronized oscillations differ in the laminar pattern of current flow that they produce in the neocortex, suggesting a differential cortical involvement.

MATERIALS AND METHODS

Sprague Dawley rats (250–350 gm) were anesthetized with ketamine–HCl (100 mg/kg, i.p.) and xylazine (5 mg/kg, i.p.). After induction of surgical anesthesia, the animal was placed in a stereotaxic frame. All skin incisions and frame contacts with the skin were injected with lidocaine (2%). A unilateral craniotomy extended over the parietofrontal cortex. Small incisions were made in the dura as necessary, at the locations of insertion of the probes. The cortical surface was covered with artificial CSF (ACSF) for the duration of the experiment. Anesthesia was supplemented with a constant (4 μl/min) intramuscular infusion of ketamine (100 mg/ml) and xylazine (5 mg/ml). Body temperature was monitored and maintained constant (36–37° C). All surgical procedures were reviewed and approved by the Animal Care Committee of McGill University.

Electrophysiological recordings. Electrophysiological recordings were performed using linear 16-channel silicon probes with 100 μm intersite spacing (Center for Neural Communication Technology, University of Michigan). To reduce and equalize the impedance (500 KΩ) of the recording sites on the silicon probes, they were oxidized before use. Current source density analyses (CSDs) were derived from the voltage recordings of the 16 channel probes as previously described (Castro-Alamancos and Connors, 1996). These probes permitted to perform CSDs on the spontaneous activity without the need of averaging. Electrophysiological responses were sampled at 5–10 kHz and stored and analyzed on a computer using Experimenter's Workbench (DataWave Technologies) and Origin Labtalk (Microcal Software) software.

Microdialysis. Drug infusions were performed using microdialysis probes. The dialysis membrane extended 2 mm in length and 200 μm in diameter (Castro-Alamancos and Borrell, 1995). ACSF was infused constantly through the microdialysis probe at a rate of 2–4 μl/min. Drugs were dissolved in the oxygenated (95% O_2 and 5% CO_2) ACSF, which consisted of (in mM): NaCl 126, KCl 3, NaH_2Po_4 1.25, $NaHCO_3$ 26, $MgSO_4$ $7H_2O$ 1.3, dextrose 10, and $CaCl_2$ $2H_2O$ 2.5.

Probe location. Microdialysis probes and silicon probes were inserted stereotactically (all coordinates given are in millimeters and refer to bregma and the dura according to the atlas of Paxinos and Watson, 1982; Fig. 1*A*). Coordinates for the thalamic microdialysis probe were approximately: anteroposterior, −2.0; lateral, 2.5. The microdialysis probe membrane extended 2 mm in depth starting at 5 mm from the dura. Coordinates for the silicon probe in neocortex were approximately: anteroposterior, 1.0; lateral, 3. Coordinates for the thalamic stimulation electrode were: anteroposterior, −2.0; lateral, 3; ventral, 6. These coordinates were chosen because they correspond to the location where thalamocortical responses are evoked in the neocortex by stimulating the ventrobasal thalamus (Castro-Alamancos and Connors, 1996). Insertion of the silicon probe into the neocortex was performed with guidance from

a surgical microscope. The recording sites on the probe were visualized, and the most dorsal site was placed 100 μm into the cortex from the surface. Also, electrical stimulation of the thalamus was used to define the location of thalamocortical-evoked current sinks and sources.

RESULTS

A microdialysis probe was inserted into the thalamus, and field recordings (1–3 kHz bandpass filters) were obtained from the neocortex (Fig. 1*A*). ACSF was continuously infused through the microdialysis probe while local field potentials were recorded in the neocortex. Fast Fourier transforms were derived from every 2 sec from field potential activity recorded from the site, located 1 mm in depth. Figure 1*B* shows the evolution of the power spectrum of neocortical activity over time displayed as a color-contour plot. The power for each frequency is color-coded so that an increase in the power is displayed as a hot color (yellow, red), and zero is displayed as blue. Under ketamine–xylazine anesthesia, slow-wave activity (~1 Hz) is prominent in neocortex (Steriade et al., 1993). When bicuculline methbromide (BMI; 400 μM) is included in the ACSF and infused into the thalamus, the cortical slow wave activity is abolished and substituted by a prominent and continuos activity at 3 Hz. The cortical activity induced by blockade of thalamic $GABA_A$ receptors consists of a negative spike followed by a positive wave. The wave component is best observed from the superficial recording sites (700 μm in depth; Fig. 1*D*). Although the 3 Hz activity is continuous, its amplitude waxes and wanes (Fig. 1*C*). Waxing and waning normally occurs without interruption of the 3 Hz activity. The same results were obtained in every such experiment conducted ($n = 7$). The spread of BMI from the probe was evaluated by recording synaptic field potential responses in neocortex (evoked by local stimulation) at different distances from the microdialysis probe while applying an AMPA receptor antagonist (CNQX; 400 μM). The AMPA receptor antagonist is known to spread at least as much as the BMI, because it blocks its effects in neocortex (Castro-Alamancos and Borrell, 1995). The results revealed that after 1 hr of CNQX infusion the evoked synaptic response was abolished at 0.5 mm from the probe, but unaffected at 1.5 mm (data not shown). This indicates that the spread of CNQX and hence of BMI is ~1 mm from the probe and largely confined to the thalamus in our experiments.

In thalamic slices, $GABA_B$ receptor antagonists abolish 3 Hz oscillations induced by $GABA_A$ receptor blockade (von Krosigk et al., 1993). Indeed, numerous experimental findings indicate that thalamic $GABA_B$ receptors play a critical role in the genesis of synchronous discharges (Huguenard and Prince, 1997). The next experiment tested the effect of blocking $GABA_B$ receptors on the 3 Hz activity induced by thalamic $GABA_A$ receptor blockade. Figure 2*A* shows that the 3 Hz activity generated by BMI application in the thalamus is completely abolished by infusing a $GABA_B$ receptor antagonist (CGP35348; 1000 μM) in the thalamus ($n = 5$). Notice that the 3 Hz activity is abolished and substituted by lower frequency activity.

During the application of BMI or BMI and CGP35348 into the thalamus, a prominent synchronous oscillatory activity at 12 Hz occurred sporadically in many experiments (Fig. 2). This activity was only observed when thalamic $GABA_A$ disinhibition was present, and it was not abolished by $GABA_B$ receptor blockade. The activity consisted of long trains (10–60 sec) of continuous discharges at 12 Hz consisting of a negative spike followed by a positive wave. Although 12 Hz discharges are observed during thalamic application of BMI alone, they tend to occur more regularly when CGP35348 is added. Figure 2 shows such an example; during application of BMI and CGP35348 into the thalamus, 3 Hz discharges are abolished and substituted by low-frequency activity. Latter, sporadic long trains of activity at 12 Hz occur. Preliminary results indicate that the conditions for the generation of these discharges are a combination of thalamic disinhibition and cortical activation. The 12 Hz discharges occur reliably when the level of anesthesia is low, and they are mostly absent during high levels of anesthesia. With the anesthetic dose used in the present study, the average interval between discharges ranged from 5 to 30 min. However, if the anesthetic supplementation is reduced by half, the average interval ranges from 3 to 10 min (based on two experiments).

The 16-site linear array silicon probes allow to record voltage through the depth of the neocortex and use it to derive CSD analyses that are displayed as color contour plots. This reveals the laminar current flow through the neocortex during the two main forms of oscillatory activity generated by thalamic disinhibition (i.e., 3 and 12 Hz discharges). Figure 3 shows a typical example of a CSD corresponding to 3 Hz activity induced by application of BMI into the thalamus. The negative spike component corresponds to a current sink (red) in upper layer VI followed by a stronger sink in layer IV that spreads very effectively to layers II–III. The upper layer VI sink is corresponded by a source (blue) in lower layer VI, whereas the layer IV sink is accompanied by a source in layer V. The positive wave component of the discharge corresponds to a propagating current source in the upper layers (from layer IV to layers II-III) and a sink in layer V. This pattern of current flow is repeated with every discharge. The locations of the layer IV and upper VI current sinks coincide with those evoked by stimulation of the ventrobasal thalamus (data not shown; see Castro-Alamancos and Connors, 1996; Kandel and Buzsaki, 1997).

Figure 4 shows a CSD analysis corresponding to a 12 Hz discharge. It reveals that in some respects the laminar current flow was quite similar to the 3 Hz activity. The initial current sink in upper layer VI was followed by a current sink in layer IV that spreads very effectively to layers II–III. A layer V source accompanied the layer IV sink. Next was a sink in layer V, and the development of a current source in the upper layers that peaked in amplitude immediately before the next upper layer sink. This delayed source coincides with the layer VI sink. Thus, although the spatial location of sinks and sources for the 3 and 12 Hz discharges was similar, their dynamics were quite distinct. This was specially the case for the upper layer current source. It occurred immediately after the upper layer sink during the 3 Hz activity, but immediately before the upper layer sink during the 12 Hz activity. Also, during the 3 Hz activity the layer VI sink had a corresponding source in lower layer VI, whereas during the 12 Hz activity the layer VI sink coincided with an upper layer source that immediately preceded the strong upper layer sink. Results displayed in Figures 3 and 4 were obtained in the same experiment.

DISCUSSION

This study reveals that block of thalamic $GABA_A$ receptors produces two prominent forms of oscillatory activity in the neocortex: 3 and 12 Hz discharges. The 3 Hz discharges, but not the 12 Hz discharges, are completely abolished by blocking thalamic $GABA_B$ receptors. Thus, functional disconnection of the nucleus reticularis of the thalamus (nRT; during $GABA_A$ and $GABA_B$ receptor blockade) abolishes the 3 Hz activity but not the 12 Hz activity, suggesting that this nucleus is not involved in the gener-

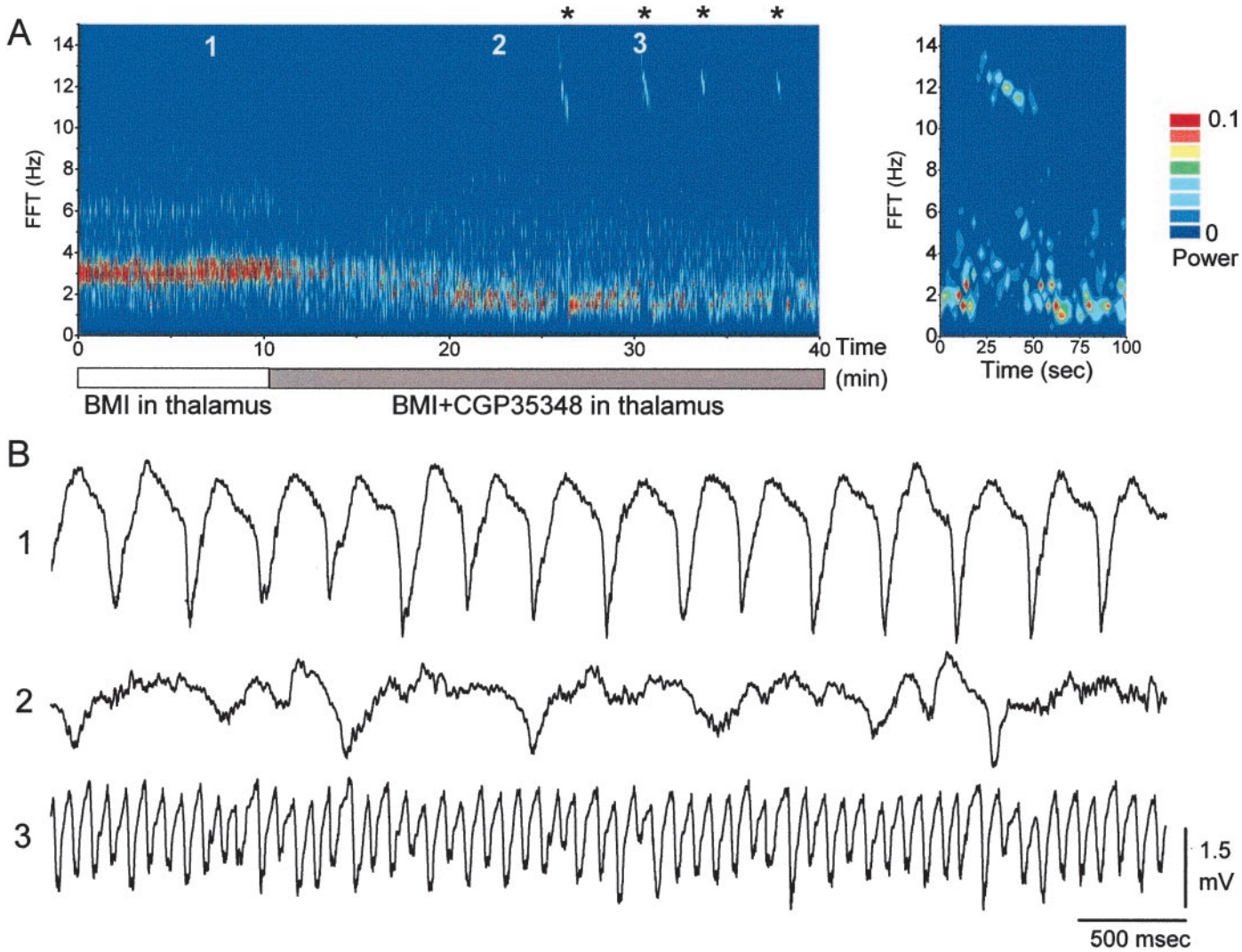

Figure 2. Effect of blocking thalamic $GABA_B$ receptors on the 3 Hz activity induced by blocking thalamic $GABA_A$ receptors. *A*, Power spectrum derived from every 2 sec of spontaneous field potential activity recorded from the neocortex and displayed as a color contour plot. During infusion of a $GABA_A$ receptor antagonist (BMI) through the microdialysis probe neocortical activity consists of synchronous activity at 3 Hz. Subsequent application of a $GABA_B$ receptor antagonist (CGP35348) completely abolishes the 3 Hz activity and substitutes it with slow-wave activity. During application of BMI alone or BMI and CGP35348, sporadic and long-lasting discharges at 12 Hz occurred. The *asterisks* mark these occurrences. The *right inset* shows a close up of the 12 Hz activity. *B*, Examples showing 3 Hz discharges (1), slow-wave activity (2), and 12 Hz discharges (3). The *numbers* on the traces correspond to the times indicated in *A*. Recordings were from a site 1 mm in depth from the surface. Traces are 5-sec-long.

ation of 12 Hz discharges. The negative spike and positive wave patterns at 3 and 12 Hz show similarities in the laminar profile of current spread. The spike component begins in upper layer VI and layer IV, with a strong spread to upper layers, whereas the wave component is characterized by a strong source in the upper layers and a sink in layer V. However, the dynamics of sinks and sources differed between the 3 and 12 Hz activities. The most prominent difference related to the position of the upper layer current source with respect to the upper layer current sink. During the 3 Hz activity, the source followed immediately after the sink, whereas during the 12 Hz activity the current source always preceded the current sink.

An important observation was that the 3 Hz activity generated by blocking thalamic $GABA_A$ receptors was completely abolished by application of a $GABA_B$ receptor antagonist in the thalamus. This finding supports an essential involvement of the nRT in the generation of the 3 Hz discharges. Indeed, lesions of the nRT abolish the synchronous discharges (i.e., high-voltage spindles) of genetically prone rats (Buzsaki et al., 1988). Also, work using thalamic slices has shown that when thalamic $GABA_A$ receptors are blocked, $GABA_B$-mediated responses are observed (von Krosigk et al., 1993; Bal et al., 1994). This seems to be caused primarily by a reduction of intra-nRT inhibition (Huntsman et al., 1999), resulting in the production of longer and higher frequency bursts in nRT neurons. Bursting in nRT produces long-lasting $GABA_B$-mediated inhibitory postsynaptic potentials in thalamic relay neurons (Kim and McCormick, 1998), resulting in rebound-bursts at ~3 Hz. Logically, blockage of thalamic $GABA_B$ receptors results in the abolition of the 3 Hz synchronous oscillatory activity.

A surprising result of thalamic disinhibition was the occurrence of 12 Hz discharges. They occurred either during $GABA_A$ receptor block or complete disinhibition. Under the conditions during which 12 Hz discharges appeared, the nRT could be functionally

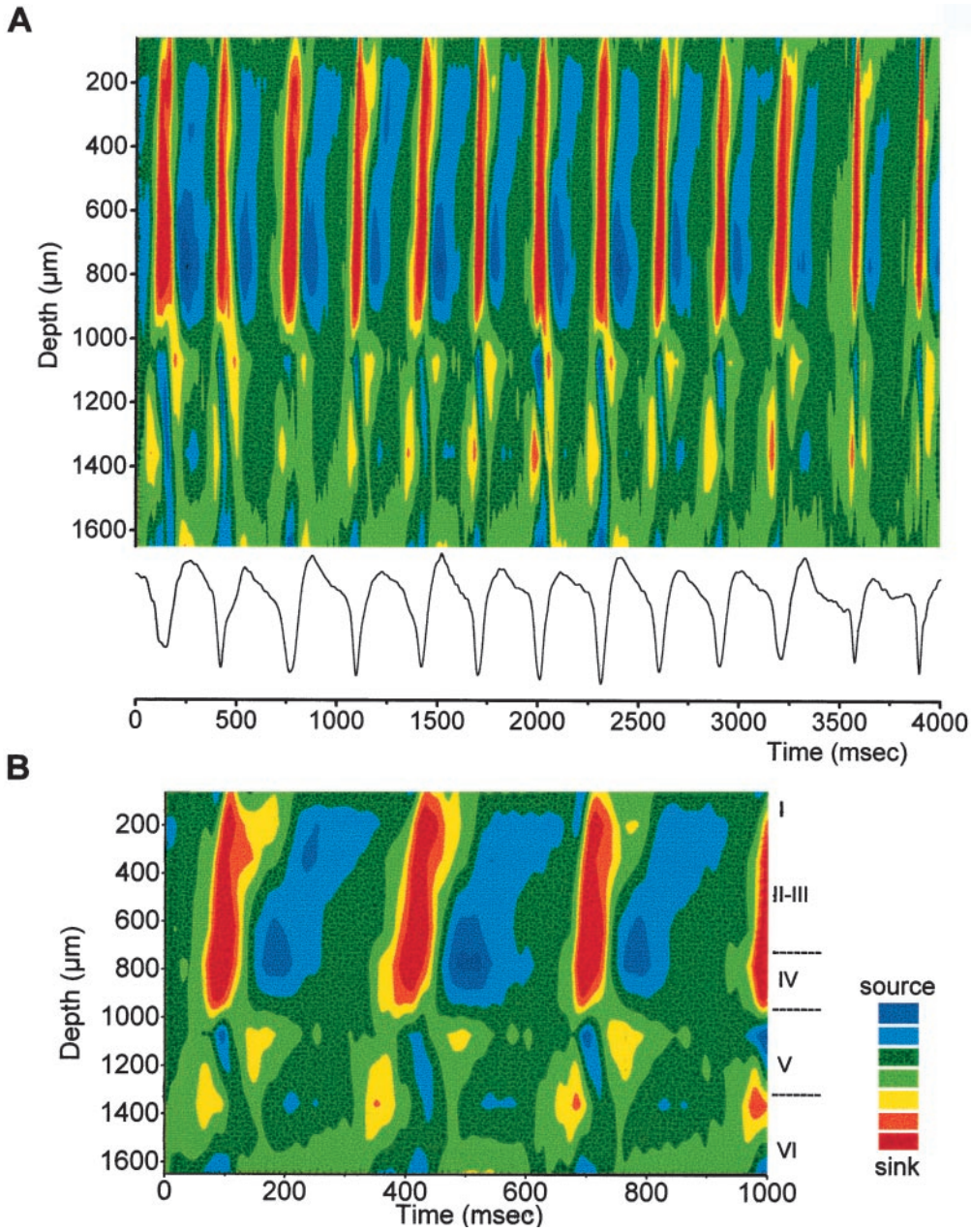

Figure 3. CSD analysis of 3 Hz synchronous discharges induced by thalamic $GABA_A$ receptor block. *A*, CSD analysis displayed as a color contour plot corresponding to 4 sec of 3 Hz discharges in the neocortex, induced by thalamic $GABA_A$ receptor block. The *bottom trace* corresponds to the field potential recorded from the site located 700 μm from the surface. In the CSD contour plots shown, hot colors (*red, yellow*) represent current sinks, cool colors (*blues*) represent current sources, and *greens* are around zero. CSDs were derived from the spontaneous activity without averaging (bandpass filter 1–3 kHz). *B*, Close up of a CSD corresponding to the same conditions as in *A*.

disconnected from the dorsal thalamus because of complete block of GABA receptors. This indicates that firing in the nRT cannot drive 12 Hz discharges. During complete thalamic disinhibition the corticothalamic–cortical loop is devoid of inhibitory control and as a result corticothalamic activity results in a direct positive feedback to the neocortex, which may facilitate the generation of 12 Hz discharges. It is interesting to note that in a rodent model of absence epilepsy (i.e., GAERS) synchronous discharges occur at ~8–11 Hz (Vergnes et al., 1990). Further work will need to explore the mechanisms responsible for the generation of 12 Hz discharges induced by thalamic disinhibition. Although, as described below, CSD analysis suggests that the neocortex may have an active role in generating this activity.

The two forms of synchronous oscillatory activity generated by thalamic disinhibition show similar patterns of laminar current flow in the neocortex corresponding to a spike and wave complex. The spike and the wave components have very different profiles. The spike component consists of a sink in upper layer VI followed by a sink in layer IV that spreads to layers II–III. The wave component consists of a sink in layer V and a prominent source in the upper layers. Previous work has shown similar patterns of current flow evoked by thalamic stimulation (Castro-Alamancos and Connors, 1996; Kandel and Buzsaki, 1997). The major difference between the CSD profiles of the 3 and 12 Hz activities was the dynamics of upper layer sinks and sources. A clear distinction was that during the 3 Hz activity, the upper layer source, corresponding to the wave component, occurred immediately after the strong upper layer sink, while in the case of the 12 Hz activity the upper layer source occurred immediately before the upper layer sink. In addition, the sinks in layer VI differed as to the location of the corresponding sources. During the 3 Hz activity, the layer VI sink displays a corresponding source in lower layer VI. However, the layer VI sink of the 12 Hz activity displays its current source in the upper layers, and this source

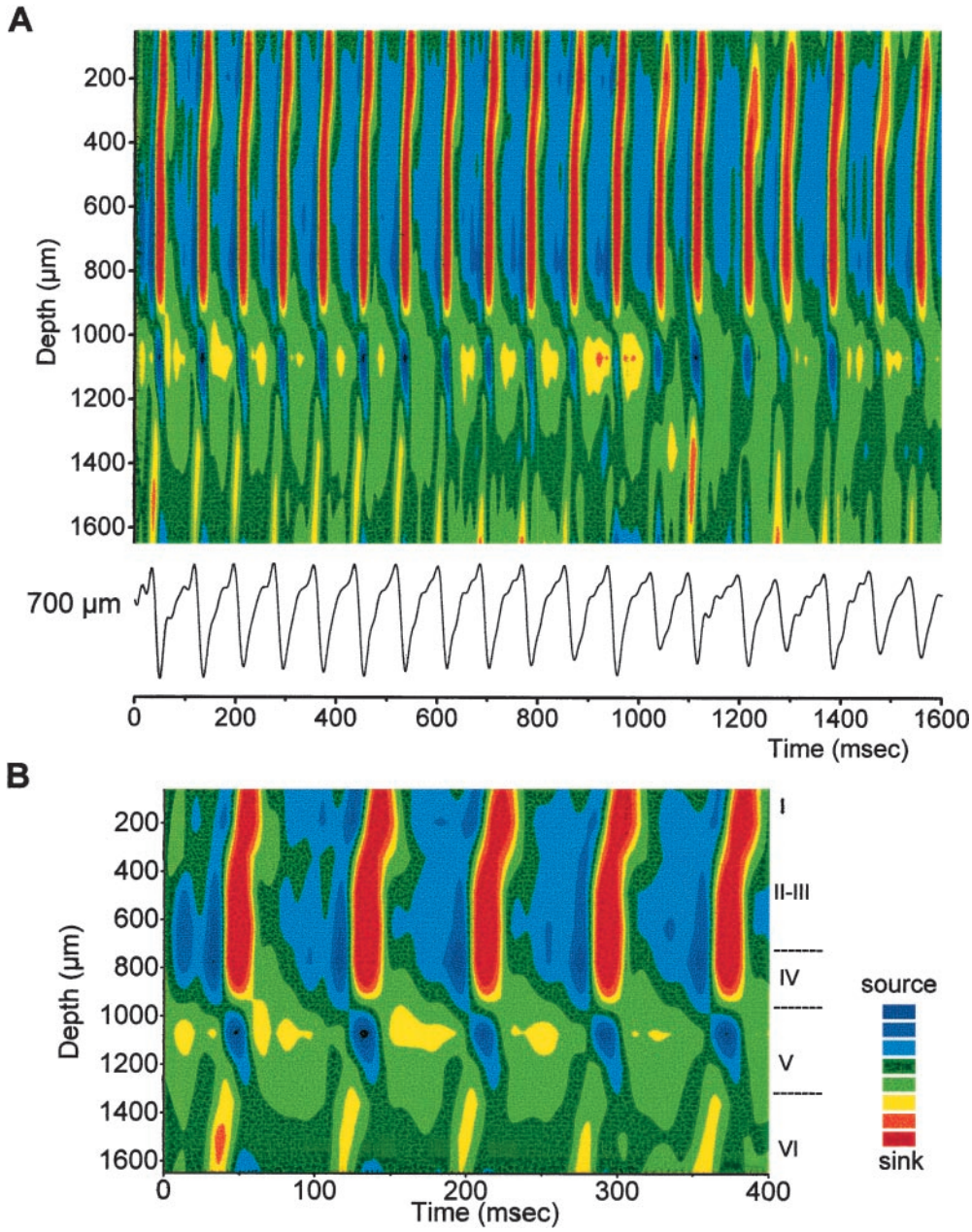

Figure 4. CSD analysis of 12 Hz discharges induced by thalamic disinhibition. *A*, CSD analysis displayed as a color contour plot corresponding to 1.6 sec of a 12 Hz discharge in the neocortex. The bottom trace corresponds to the field potential recorded from the site located 700 μm from the surface. In the CSD contour plots shown, hot colors (*red, yellow*) represent current sinks, cool colors (*blues*) represent current sources, and *greens* are around zero. CSDs were derived from the spontaneous activity without averaging (bandpass filter 1–3 kHz). *B*, Close up of a CSD corresponding to the same conditions as in *A*.

immediately precedes the large upper layer sink. These results suggest differences in the contribution of the neocortex to both types of activity. Thus, the current flow during the 3 Hz activity is similar to the pattern of cortical current flow generated by thalamic stimulation (Castro-Alamancos and Connors, 1996; Kandel and Buzsaki, 1997). However, during 12 Hz discharges the current flow is incompatible with a simple response of the neocortex to thalamic input. This is evidenced by the fact that cortical activity is present before the large upper layer sink. Possibly, cortical activation during thalamic disinhibition may account for the occurrence of 12 Hz discharges.

In anesthetized cats, there is evidence of inactivity within large numbers of thalamic neurons during spontaneously occurring seizures and these seizures occur even after thalamectomy, indicating that the neocortex alone can generate these discharges without thalamic involvement (Steriade and Contreras, 1995, 1998). Instead of these spontaneous paroxysmal developments typical of cats, rats display spontaneous synchronous oscillations, called high-voltage spindles (Buzsaki et al., 1988), which are similar to the 3 Hz discharges observed in the present study after thalamic BMI. The occurrence of high-voltage spindles seem to depend on many variables, such as sex, strain, and anesthesia (Buzsaki et al., 1991; Jando et al., 1995). Future work will have to establish if the effects of thalamic $GABA_A$ receptor blockade described here are independent of these variables.

The present study found that blockade of thalamic $GABA_A$ receptors *in vivo* produces continuos waxing and waning of synchronized oscillations at 3 Hz that depend on thalamic $GABA_B$ receptors and sporadic synchronized oscillations at 12 Hz that do not depend on thalamic $GABA_B$ receptors. Both forms of synchronized oscillations differ in the laminar pattern of current flow that they produce in the neocortex, suggesting a differential cor-

tical involvement. In conclusion, intrathalamic inhibitory processes play an essential role in the generation of neocortical synchronized oscillatory activity that may be related to certain forms of generalized seizures.

REFERENCES

Bal T, von Krosigk M, McCormick DA (1994) From cellular to network mechanisms of a thalamic synchronized oscillation. In: Temporal coding in the brain (Buzsaki G, Singer W, Berthoz A, Christen Y, eds). Berlin: Springer. pp.129–144.

Buzsaki G, Bickford RG, Ponomareff G, Thal LJ, Mandel R, Gage FH (1988) Nucleus basalis and thalamic control of neocortical activity in the freely moving rat. J Neurosci 8:4007–4026.

Buzsaki G, Kennedy B, Solt VB, Ziegler M (1991) Noradrenergic control of thalamic oscillation: the role of α-2 receptors. Eur J Neurosci 3:222–229.

Castro-Alamancos MA, Borrell J (1995) Contribution of NMDA and non-NMDA glutamate receptors to synchronized excitation and cortical output in the primary motor cortex of the rat. Brain Res Bull 37:539–543.

Castro-Alamancos MA, Connors BW (1996) Spatiotemporal properties of short-term plasticity in sensorimotor thalamocortical pathways of the rat. J Neurosci 16:7742–7756.

Gloor P, Fariello RG (1988) Generalized epilepsy: some of its cellular mechanisms differ from those of focal epilepsy. Trends Neurosci 11:63–68.

Gloor P, Quesney LF, Zumstein H (1977) Pathophysiology of generalized penicillin epilepsy in the cat: the role of cortical and subcortical structures. II. Topical application of penicillin to the cerebral cortex and to subcortical structures. Electroencephalogr Clin Neurophysiol 43:79–94.

Gloor P, Avoli M, Kostopoulos G (1990) Thalamo-cortical relationships in generalized epilepsy with bilaterally synchronous spike and wave discharge. In: Generalized epilepsy, neurobiological approaches (Avoli M, Gloor P, Kostopoulos G, Naquet R eds), pp 190–112. Verlag: Birkhauser.

Huguenard JR, Prince DA (1997) Basic mechanisms of epileptic discharges in the thalamus. In: Thalamus, Vol II (Steriade M, Jones EG, McCormick DA eds), pp 295–330. Amsterdam: Elsevier.

Huntsman MM, Porcello DM, Homanics GE, DeLorey TM, Huguenard JR (1999) Reciprocal inhibitory connections and network synchrony in the mammalian thalamus. Science 283:541–543.

Jando G, Carpi D, Kandel A, Urioste R, Horvath Z, Pierre E, Vadi D, Vadasz C, Buzsaki G (1995) Spike-and-wave epilepsy in rats: sex differences and inheritance of physiological traits. Neuroscience 64:301–317.

Jasper HH, Kershman J (1941) Electroencephalographic classification of the epilepsies. Arch Neurol Psychiatr 45:903–943.

Kandel A, Buzsaki G (1997) Cellular-synaptic generation of sleep spindles, spike-and-wave discharges, and evoked thalamocortical responses in the neocortex of the rat. J Neurosci 17:6783–6797.

Kim U, McCormick DA (1998) The functional influence of burst and tonic firing mode on synaptic interactions in the thalamus. J Neurosci 18:9500–9516.

Paxinos G, Watson C (1982) The rat brain in stereotaxic coordinates. New York: Academic.

Prince DA, Farrell D (1969) "Centrencephalic" spike-wave discharges following parenteral penicillin injection in the cat. Neurology 19:309–310.

Ralston B, Ajmone-Marsan C (1956) Thalamic control of certain normal and abnormal cortical rhythms. Electroenceph. Clin. Neurophysiol. 8:559–582.

Steriade M, Contreras D (1995) Relations between cortical and thalamic cellular events during transition from sleep patterns to paroxysmal activity. J Neurosci 15:623–642.

Steriade M, Contreras D (1998) Spike-wave complexes and fast components of cortically generated seizures. I. Role of neocortex and thalamus. J. Neurophysiol 80:1439–1455.

Steriade M, Nunez A, Amzica F (1993) A novel slow (<1 Hz) oscillation of neocortical neurons in vivo: depolarizing and hyperpolarizing components J Neurosci 13:3252–3265.

Vergnes M, Marescaux Ch, Depaulis A, Micheletti G, Warter J-M (1990) Spontaneous spike-and-wave discharges in Wistar rats: a model of genetic generalized convulsive epilepsy. In: Generalized epilepsy, neurobiological approaches (Avoli M, Gloor P, Kostopoulos G, Naquet R eds), pp 238–253. Verlag: Birkhauser.

von Krosigk M, Bal T, McCormick DA (1993) Cellular mechanisms of a synchronized oscillation in the thalamus. Science 261:361–364.